International Journal of Pharmaceutics 404 (2011) 308–316

Contents lists available at ScienceDirect

International Journal of Pharmaceutics

journal homepage: www.elsevier.com/locate/ijpharm

Pharmaceutical Nanotechnology

Photosensitizer loaded HSA nanoparticles II: *In vitro* investigations

Annegret Preuß[a], Kuan Chen[a], Steffen Hackbarth[a], Matthias Wacker[b], Klaus Langer[c], Beate Röder[a,*]

[a] Department of Physics, Humboldt - Universität zu Berlin, Newtonstraße 15, 12489 Berlin, Germany
[b] Department of Pharmaceutical Technology, Goethe-Universität Frankfurt am Main, Max-von-Laue -Str. 9, 60438 Frankfurt am Main, Germany
[c] Department of Pharmaceutical Technology and Biopharmacy, Westfälische Wilhelms-Universität Münster, Corrensstr. 1, 48149 Münster, Germany

ARTICLE INFO

Article history:
Received 30 July 2010
Received in revised form 9 November 2010
Accepted 12 November 2010
Available online 19 November 2010

Keywords:
PDT
Nanocarrier
Singlet oxygen generation
Human serum albumin
Phototoxicity
Biodegradability

ABSTRACT

The photosensitizing efficiency of human serum albumin (HSA) nanoparticles loaded with the photosensitizers meta-tetra(hydroxy-phenyl)-chlorin (mTHPC) and meta-tetra(hydroxy-phenyl)-porphyrin (mTHPP) was investigated *in vitro*. The endocytotic intracellular uptake, and the time dependent drug release caused by nanoparticle decomposition of the PS loaded HSA nanoparticles were studied on Jurkat cells in suspension. The photoxicity as well as the intracellular singlet oxygen ($^1O_2$) generation were investigated in dependence on the incubation time. The obtained results show that HSA nanoparticles are promising carriers for the clinical used mTHPC (Foscan). After release the ($^1O_2$) generation as well as the phototoxicity are more efficient compared with mTHPC applied without the HSA nanoparticles.

1. Introduction

Photodynamic therapy (PDT) is an alternative method to treat tumors and other diseases (Röder, 2000; Dougherty et al., 1998; Amato, 1993).

Photodynamic treatment is based on the presence of a drug with photosensitizing properties combined with light and oxygen (Dougherty et al., 1998; Henderson and Dougherty, 1992). In darkness photosensitizer (PSs) exhibit no or low toxicity. The absorption of light with suitable wavelength by the tumor-localized PS molecules leads to the generation of highly toxic singlet oxygen ($^1O_2$) (Foote, 1968). This species causes cell death via direct or indirect pathways. One big advantage of this method is the controlled photodamage of cells by variation of dose and duration of irradiation with visible light.

The application of PSs without carriers causes some problems. First, the PSs can become active before they reach the target cells. Second the long time used "selectivity" caused by different metabolisms of PSs in normal and tumor cells is not satisfying.

In general two different mechanisms can be used for carrier mediated tumor targeting: the active targeting uses specific molecules that bind to the target cells (e.g. monoclonal antibodies) or passive targeting using the enhanced permeability and retention (EPR) effect. Nowadays it is accepted that the EPR effect allows a very efficent passive targeting of tumor tissue *in vivo* (Maeda et al., 2001; Maeda, 1994; Matsamura and Maeda, 1986; Duncan and Sat, 1998; Perrault et al., 2009).

Taking into account that PSs of the type, investigated here, are uptaken by cells, their intracellular localization plays an important role for the efficiency of the photodynamic effect.

For this reason, beside phototoxicity we investigated the uptake and the intracellular distribution after release of meta-tetra(hydroxy-phenyl)-chlorin (mTHPC) and meta-tetra(hydroxy-phenyl)-porphyrin (mTHPP) from the human serum albumin (HSA) nanoparticles administered to cells *in vitro* as potential carriers for passive tumor targeting.

Nanoparticles are regarded as potential PDT drug carrier systems (Jux and Röder, 2010) because of their high stability, high carrier capacity, feasibility to carry both hydrophobic and hydrophilic agents (Gelperina et al., 2005), as well as the possibility of multiple administration methods (oral or injection). Because of the EPR effect nanoparticles with suitable size (at least 40 kDa, Maeda et al., 2001) preferentially accumulate in tumor tissue. This makes them very interesting for design of controllable drug release carriers. In this work particles of a size of approximately 200 nm were used with regard to further *in vivo* application.

Abbreviations: CLSM, confocal laser scanning microscopy; EPR, enhanced permeability and retention; FCS, fetal calf serum; FLIM, fluorescence lifetime imaging; HSA, human serum albumin; mTHPC, meta-tetra(hydroxy-phenyl)-chlorin; mTHPP, meta-tetra(hydroxy-phenyl)-porphyrin; PBS, phosphate buffered saline; PDT, photodynamic therapy; PS, photosensitizer; $^1O_2$, singlet oxygen.

* Corresponding author.
E-mail address: roeder@physik.hu-berlin.de (B. Röder).

0378-5173/$ – see front matter © 2010 Elsevier B.V. All rights reserved.
doi:10.1016/j.ijpharm.2010.11.023

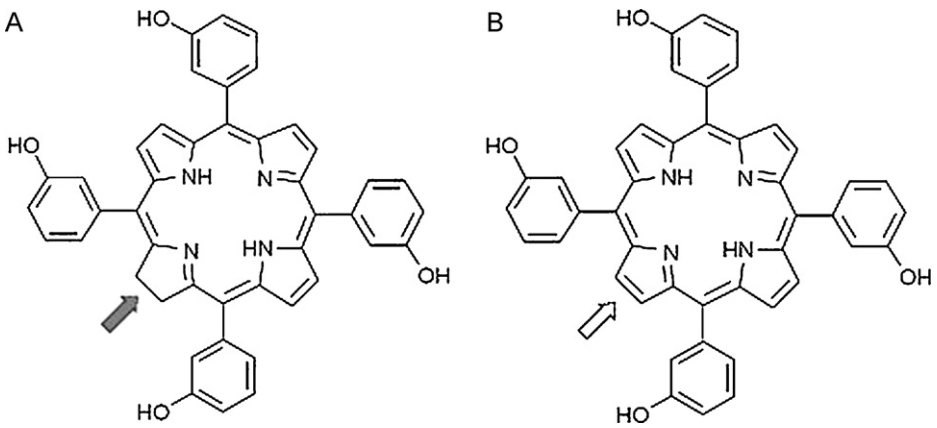

Fig. 1. Chemical structure of (A) meta-tetra(hydroxy-phenyl)-chlorin (mTHPC) and (B) meta-tetra(hydroxy-phenyl)-porphyrin (mTHPP).

Nanoparticular formulations consisting of HSA have been established as carriers for different drugs like cytostatics (Dreis et al., 2007). In this paper we report about *in vitro* investigations on the capability of HSA nanoparticles as carriers for the 2nd generation PS mTHPC (Marchal et al., 2004; Leung et al., 2002; Ma et al., 1994) and the 1st generation PS mTHPP (see Fig. 1).

HSA-based nanoparticles, which were prepared as described in (Langer et al., 2008) have a defined particle diameter between 100 and 300 nm with a narrow size distribution (Langer et al., 2000, 2008).

In a former work we described their potential as drug carrier for pheophorbide a. We reported about the photophysical properties of pheophorbide a-HSA nanoparticles as well as their photocytotoxicity in Jurkat cells (Chen et al., 2009).

These principle investigations were carried out without variation of different HSA-parameters or PS loading. In a next step we investigated the photophysical properties of mTHPC-HSA nanoparticles in dependence on loading ratio and degree of HSA glutaraldehyde cross linking (Chen et al., 2010). These experiments were done to switch on one hand to a clinical used PS (Dougherty et al., 1998; Bonnett et al., 1989; Copper et al., 2003; Hopper et al., 2004) and to investigate the influence of different parameters of HSA nanoparticles on the efficiency of phototoxicity.

Here we report about a comparative study on the HSA nanoparicle accumulation using two different PSs, the intracellular drug release and phototoxicity in dependence on incubation time. The preparation and the photophysical properties of the investigated nanoparticular PS delivery systems are reported in Wacker et al. (2010).

Porphyrin based photosensitizers like mTHPC and mTHPP are interacting with cellular organells like mitochondria, Golgi or lysosomes (Paul et al., 2002, 2003; Rancan et al., 2005a; Roeder et al., 2006). Thus, to accomplish an effective photosensitization intracellular uptake of the PS molecules into the target cells is necessary. Nanoparticular drug carrier system are assumed to pass the cytoplasmatic membrane via endocytosis (Chen et al., 2009; Roeder et al., 2004). Following the intracellular pathway of endocytosis the nanoparticles are taken up into the lysosomes (Willingham and Pastan, 1984) where the biodegradable HSA carrier system is decomposed and as a result releases the PS (Chen et al., 2009).

To investigate the endocytotic uptake, the nanoparticle degradation and the following drug release Confocal Laser Scanning Microscopy (CLSM) and Fluorescence Lifetime Imaging (FLIM) were used. The intracellular uptake of the PS loaded nanoparticles in Jurkat cells was quantified by measuring the fluorescence intensity of the PS in the cell extract.

The photodynamic treatment of cancer cells with mTHPP and mTHPC causes different cell death pathways. The main mechanism is apoptosis (Oleinick et al., 2002; Kessel and Luo, 1998; Rancan et al., 2005b).

The photo- and dark toxicity of the PS loaded nanoparticles were studied in comparison with the free PS in order to judge the efficiency of the drug carrier system *in vitro*. To characterize the phototoxic effect of the PS loaded nanoparticles and to discriminate possible differences of cell death mechanism compared with the free PS, both the rate of necrosis and apoptosis were determinated separatly.

The ability of the PS to generate $^1O_2$ in its intracellular microenvironment is an important condition for an efficient photosensitization. Thus, we measured the intracellular $^1O_2$-luminescence with a high-sensitive setup as reported in Schlothauer et al. (2008). For these investigations cells in suspension are needed. Therefore, Jurkat cells, a suspension cell line, were used for all investigations.

2. Materials and methods

2.1. Samples

The HSA-nanoparticles were investigated in Jurkat cells, as well as the free PS without nanoparticles (see Table 1).

2.2. Preparation of mTHPC and mTHPP loaded HSA nanoparticles

The samples were prepared according to the established method previously described in part I (Wacker et al., 2010).

In principle, preformed HSA nanoparticles were loaded with photosensitizers in ethanol 33.3% [V/V] after addition of 2% [m/V] of dissolved HSA for mTHPC and 1.5% [m/V] for mTHPP. After 2 h of incubation time particles were purified by three steps of centrifugation (20817 g, 15 °C, 10 min) and redispersion in purified water.

Table 1
Investigated PSs and PS loaded nanoparticles, the preparation and the photophysical characterisation of the investigated nanoparticles is described in part I (Wacker et al., 2010).

Name of sample	Description
mTHPC	Meta-tetra(hydroxy-phenyl)-chlorin (see Fig. 1A)
mTHPP	Meta-tetra(hydroxy-phenyl)-porphyrin (see Fig. 1B)
mTHPC-HSA	HSA-nanoparticles, HSA monomers cross-linked by glutaraldehyde bridges (gb). The particles are saturated by 100% with gb The particles are adhesive loaded with mTHPC. Loading ratio: 20.71 μg/mg mTHPC/HSA
mTHPP-HSA	HSA – nanoparticles, HSA monomers cross-linked by gb. The HSA particles are saturated by 100% with gb. The particles are adhesive loaded with mTHPP. Loading ratio: 20.50 μg/mg mTHPP/HSA

Afterwards the particle size and polydispersity index were measured by photon correlation spectroscopy. The nanoparticle concentration (mg/mL) and photosensitizer concentration (μg/mL) were determined according to the protocol described in part I of these experimentes by (Wacker et al., 2010). The particle content is determined gravimetrically and the photosensitizer concentration photometrically after enzymatic degradation of the particle system. The loading ratio is calculated as the quotient of the photosensitizer concentration and the particle concentration (μg/mg) in the prepared suspension.

For all cell culture experiments the samples were prepared in phosphate buffered saline (PBS).

2.3. Cell culture and incubation conditions

For *in vitro* experiments, Jurkat cells (clone E 6-1 human acute T-cell leukaemia) were cultured in RPMI 1640 medium with L-glutamine supplemented with 10% fetal calf serum (FCS), 100 U/mL of penicillin and 100 μg/mL of streptomycin without phenol red (PAA). Cells were cultivated at 37 °C in 100% humidity and 5% CO_2 and were seeded in new medium every 2–3 days (Rancan et al., 2005a; Chen et al., 2009). For all *in vitro* experiments Jurkat cells were incubated for 1 h, 3 h, 5 h, and 24 h with mTHPC, mTHPP or PS loaded nanoparticles.

The cell growth medium contains 3 μM of the PS. The 1 mM ethanol stock solutions of mTHPC and mTHPP are diluted with PBS 1:10 very slowly to prevent dye aggregation, before adding it to the medium. The resulting ethanol concentration in the medium is 0.3%. In former studies it has been shown that a concentration of ethanol up to 0.5% in the medium does not affect cell growth or health. Cells were incubated at 37 °C in 100% humidity, 5% CO_2 and in darkness.

2.4. Intracellular uptake

Intracellular uptake of PS was investigated using steady-state fluorescence spectroscopy. The incubation volume was 10 mL per sample. After different incubation times the cells were harvested, counted using a hemocytometer (about 3×10^5 cells/mL), centrifuged (room temperature, 350 g, 5 min) and washed twice with PBS. The cell pellets were frozen and stored at −20 °C for more than 20 min to break the cell membranes. For each sample, 1000 μl ethanol was added to the frozen cell pellets to extract PS molecules taken up by cells. After resuspension by ultrasonication for 5 min, the samples were centrifuged (room temperature, 5000 × g, 2 min) in order to separate the cell debris from ethanol solution.

The steady-state fluorescence was measured to calculate the amount of intracellular PS taken up by the cells. 0.1 μM, 0.2 μM, 0.5 μM, and 1.0 μM PS-ethanol solution were taken as fluorescence standard. For the calculation (1) of the intracellular concentration the average cell diameter (10 μm) was obtained in the confocal laser scanning microscope. All samples were excited at λ_{ex} = 405 nm.

$$c^{\text{uptake}} = \frac{c^{\text{extract}} \times V^{\text{extract}}}{V^{\text{cell}} \times n^{\text{cell}}} \quad (1)$$

c^{uptake} = Intracellular PS concentration; c^{extract} = PS concentration in the ethanol extract measured by fluorescence intensity; V^{extract} = volume of the enthanol extract; V^{cell} = cell volume (assumed as spherical); n^{cell} = cell number.

2.5. Dark toxicity and phototoxicity

For incubation, 1 mL of Jurkat cell suspension for each sample was placed on a 24-well plate (~2×10^5 cells/mL). The intact and dead cells were counted using a hemocytometer under an inverse microscope CKX 41 (Olympus, Hamburg). Necrotic and apoptotic cells were counted separately. Trypan Blue (Sigma) was used to indicate the necrotic cells. Apoptotic cells were distinguished by their dramatic changes in cell shape (see Fig. 2)

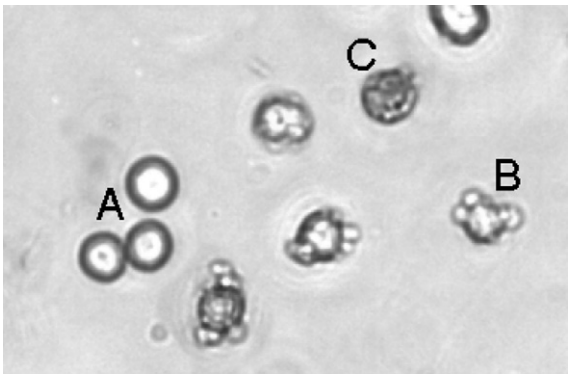

Fig. 2. Photosensitized and Trypan Blue stained Jurkat cells were photographed 2 h after irradiation using a light microscope (×200). (A) Intact cell, (B) apoptotic cell with prominent membrane blebbing and changes in shape, and (C) necrotic cells.

In dark toxicity tests the intact and dead cell numbers were counted after incubation. In phototoxicity tests the cells were washed with fresh RPMI 1640 medium (room temperature, 350 g, 3 min), then placed in a black 96-well culture plate with transparent bottom (250 μL, ~2×10^5 cells/mL). For irradiation a laser diode with emission at 660 nm was used as light source. The irradiation time was 120 s, which results in a light dose of 280 mJ/cm^2. The living and dead cell numbers were counted after additional 2 h of incubation. As shown in former studies for Jurkat cells the method to determine the rate of apoptotic cells via cell counting results in similar rates as the Caspase-Glo® 3/7 – Assay (Promega, Madison, USA) (Chen et al., 2009).

2.6. Drug release and intracellular distribution

The drug release and intracellular distribution were detected by fluorescence lifetime imaging FLIM and CLSM.

For incubation, 1 mL of Jurkat cell suspension for each sample was placed on a 24-well plate (~2×10^5 cells/mL). For CLSM experiments 1 μM (0.5 μL) of LysoSensor green (pH dependent fluorescence label for lysosomes and endosomes) DMSO solutions (Molecular ProbesTM, Invitrogen) were injected into Jurkat cell suspensions followed by 20 min incubation for PS-fluorescence label colocalization. For all samples at least four cells were imaged. One representive image per sample is shown.

The cell images were observed with a CLSM (FluoViewTM FV1000, Olympus) with FLIM-extension (Pico Quant, Berlin). mTHPP, mTHPC and LysoSensor green were excited with a laser diode at λ_{ex} = 405 nm for imaging and excited with a nanosecond pulse laser at λ_{ex} = 440 nm for fluorescence lifetime measurements. The fluorescence of LysoSensor was recorded at λ_{em} = 520 nm, and mTHPP, and mTHPC at λ_{em} = 650 nm. No auto-fluorescence from HSA nanoparticles or cellular structures were observed in the range of measurement wavelength.

2.7. Intracellular $^1O_2$ generation and triplet lifetime

The ability of the PS to generate $^1O_2$ in its intracellular microenvironment is an important condition for an efficient photosensitization. Thus, a new setup to investigate the intracellular $^1O_2$ generation was built in our group (Schlothauer et al., 2008).

The Jurkat cells were incubated for 5 h with 3 μM mTHPP, mTHPC and mTHPP- and mTHPC-loaded HSA nanoparticles in darkness. Then cells were washed twice with PBS. The cell suspension

was illuminated with a YAG-pumped dye laser after washing. For mTHPP and mTHPP-HSA nanoparticles, the irradiation wavelength is 532 nm. For mTHPC and mTHPC-HSA nanoparticles the irradiation wavelength is 652 nm. The cell suspension was illuminated for 20 s. During this time, the average irradiation power was 500 μW. The $^1O_2$ luminescence of PS located inside Jurkat cells was determined with the equipment described in Schlothauer et al. (2008). The intensity of the $^1O_2$ luminescence can be calculated using Eq. (2) (Oelckers et al., 1999) where $I(t)$ is the intensity of $^1O_2$ luminescence, A is a constant that depends on several setup parameters and on the solvent. It also relates to k_Δ the $^1O_2$ luminescence rate constant. τ_Δ is the $^1O_2$ luminescence lifetime and τ_T is the triplet state lifetime of PS.

$$I(t) = A \cdot \left[\exp\left(-\frac{t}{\tau_\Delta}\right) - \exp\left(-\frac{t}{\tau_T}\right)\right] \cdot \frac{\tau_\Delta}{\tau_\Delta - \tau_T} \quad (2)$$

3. Results and discussion

3.1. Intracellular uptake

One question was if the PS will be uptaken by the cells or not using HSA nanoparicles as carriers. As could be seen from CLSM images (see Fig. 4, Section 3.2) no PS molecules are located at the cell surface. For all samples only intracellular PS fluorescence was observed. Therefore we could be sure starting our investigation on intracellular uptake, that we evaluate exclusively intracellular located PSs.

The intracellular PS concentration in Jurkat cells depending on the incubation time was determined to evaluate the efficiency of the HSA nanoparticles as drug carrier systems. These experiments were carried out in comparison to the accumulation of the free PS mTHPP and mTHPC, which are known as membrane-permeable (data shown in Fig. 3).

The intracellular uptake of both PS without HSA nanoparticles is similar after 24 h of incubation. The intracellular concentration is 1.2 μM ± 0.1 μM for mTHPP and 1.3 μM ± 0.3 μM for mTHPC. But after 1 h and 3 h of incubation with mTHPP the intracellular concentration is more than twice as high as after incubation with mTHPC.

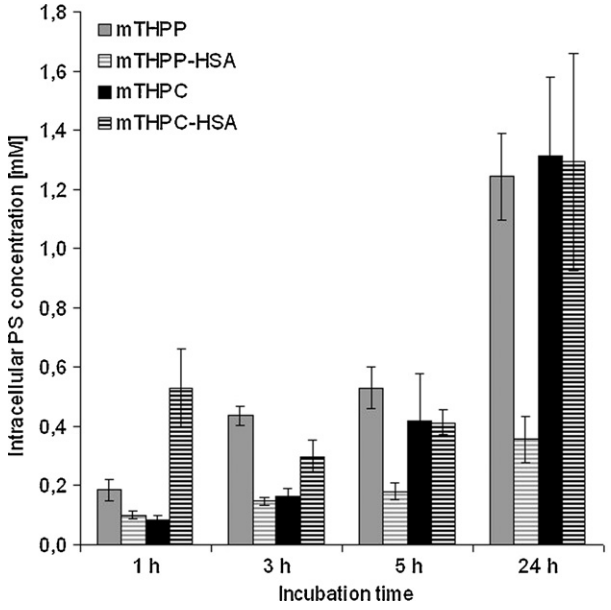

Fig. 3. Intracellular uptake of 3 μM mTHPP, mTHPP-HSA, mTHPC, mTHPC-HSA by Jurkat cells at different incubation times. The experiments were repeated twice and for each measurement the cell number was counted three times to get an average. Error bars represent the standard deviation ($n = 6$).

In contrast to the uptake of free PS the uptake of the mTHPC-HSA nanoparticles is much more efficient than the uptake of the mTHPP loaded HSA nanoparticles. After 24 h the amount of intracellular mTHPC applied by HSA nanoparticles is similar to free mTHPC and free mTHPP. The intracellular PS concentration in case of mTHPC-HSA nanoparticle application is 1.3 μM ± 0.4 μM in contrast to the low concentration for mTHPP-HSA nanoparticles 0.4 μM ± 0.1 μM. After 5 h of incubation the intracellular PS concentration of mTHPC-HSA nanoparticles is already significantly higher than for mTHPP-HSA nanoparticles.

The intracellular PS concentration of mTHPC and mTHPC-HSA nanoparticles after 5 h and 24 h incubation is similar. In contrast the uptake of mTHPP-HSA nanoparticles is significantly lower than that of free mTHPP at all incubation times.

The loading ratio of the HSA nanoparticles with the two PS is nearly the same. Therefore using a PS concentration of 3 μM in the medium, the amount of nanoparticles in the samples should be the same. If so the two PS themselves must have an impact on the endocytotic uptake of the nanoparticles. Probably this is caused by interactions between mTHPP/mTHPC loaded on HSA nanoparticles with cellular components. These interactions should be different from those of the free PS with the components of the cells during the membrane permeation.

3.2. Monitoring the endocytotic uptake of the nanoparticles and the drug release via CLSM

To be certain the PS loaded HSA nanoparticles are taken up as a whole and the PS release occurs inside of the cells, monitoring of endocytosis is necessary. Since the PS do not show fluorescence during their immobilisation on the nanoparticles (Wacker et al., 2010) an appearing and increasing fluorescence signal reports about the PS release from the nanoparticles. This fact was used to study the localization of mTHPP and mTHPC in lysosomes depending on the incubation time receiving information about the process of lysosomal nanoparticle destruction and the subsequent drug release.

As can be seen from the colocalization experiment (see Fig. 4) mTHPP applied without using nanoparticles does not accumulate in lysosomes. The mTHPP molecules pass the cytoplasmic membrane directly into the cytoplasma, thus no localization in the lysosomes is observed. After 1 h, 3 h, and 5 h of incubation for the mTHPP-HSA nanoparticles treated cells a strong overlap of the LysoSensor and mTHPP fluorescence was observed. After 24 h the mTHPP carried by HSA nanoparticles can be found in a high amount in lysosomes but also mTHPP fluorescence was observed in the cytoplasm. The images show the beginning mTHPP release from the nanoparticles after 24 h incubation.

After 1 h and 3 h of incubation with mTHPC applied without nanoparticles the cells show PS localization in lysosomes and in the cytoplasm as well unlike the mTHPP incubated cells. After 5 h and 24 h incubation no mTHPC fluorescence in the lysosomes was observed. The high affinity of mTHPC to proteins like bovine serum albumin contained in the cell growth medium is well-known (Leung et al., 2002; Sasnouski et al., 2005). Therefore it can be suggested that not all of the mTHPC passes the cytoplasmic membrane directly as some is taken up by the cells attached to proteins via endocytosis (Bento-Abreu et al., 2009; Tabernero et al., 2002). This behaviour causes the lysosomal localization of free mTHPC in the first hours of incubation.

Compared to the cells treated with free mTHPC after 1 h of incubation the mTHPC-HSA nanoparticle treated cells show significant PS localization in lysosomes. After 3 h of incubation with mTHPC-HSA nanoparticles the mTHPC localization in lysosomes is still visible but mTHPC fluorescence in the cytoplasma was observed as well. At longer incubation times with mTHPC-HSA nanoparti-

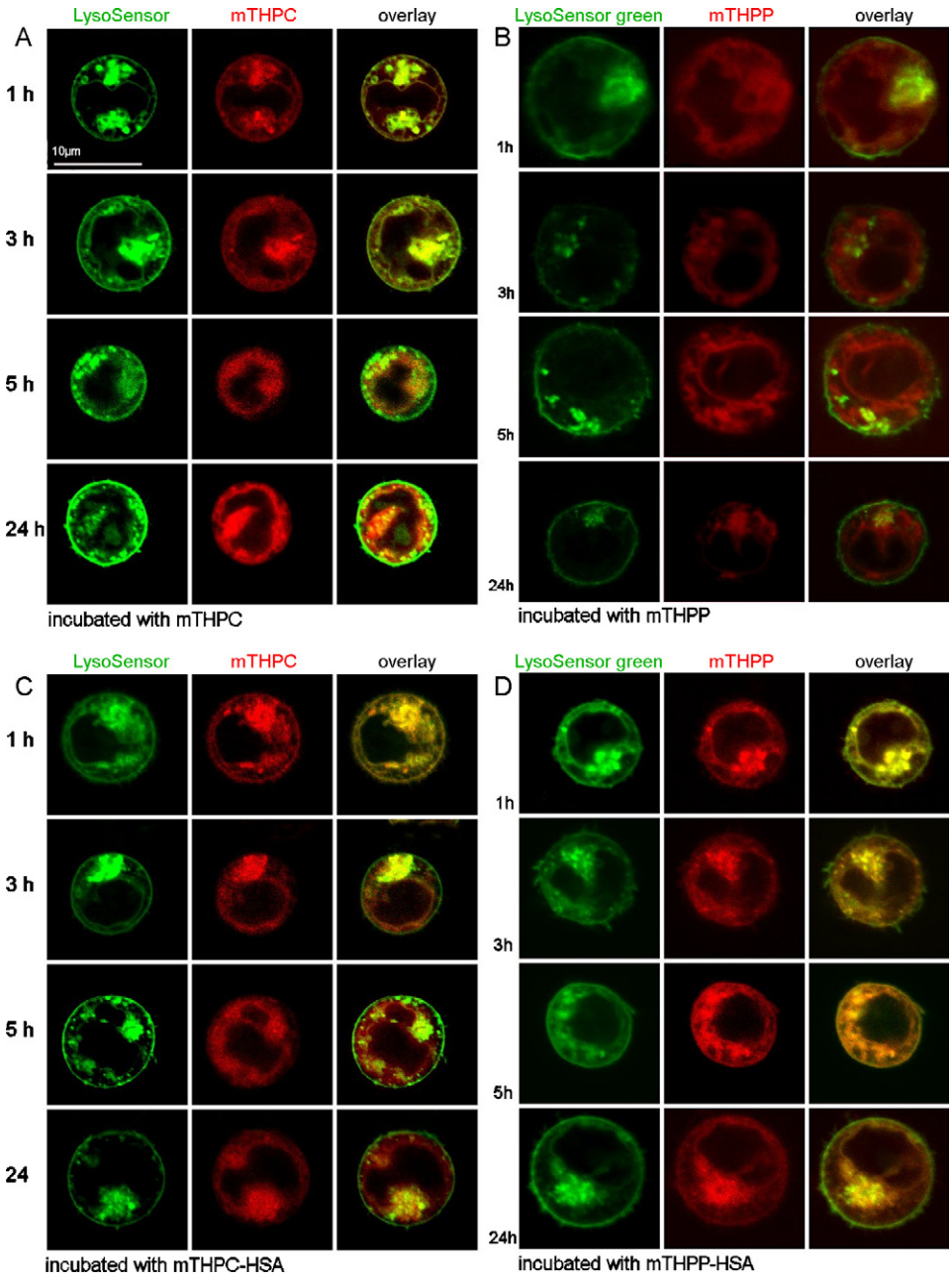

Fig. 4. PS localization in lysosomes after different incubation times, green: LysoSensor; green and red: mTHPP. Localization, as an overlap of both mTHPP and fluorescence probes is indicated by the yellow regions. The Jurkat cells were incubated with mTHPC (A), mTHPP (B), mTHPC-HSA nanoparticles (C) and mTHPP-HSA nanoparticles (D). For all samples at least four cells were imaged, one repre-sentive image per sample is shown.

cles almost no PS localization in lysosomes could be varified by fluorescence (see Fig. 4).

3.3. Investigation of drug release using FLIM

In general information about the microenvironment of fluorophors, in this case of the PS molecules, can be obtained from fluorescence lifetime changes.

The decomposition of the HSA nanoparticles and the resulting PS release should cause changes in the PS micro environment, resulting in different fluorescence decay times. Therefore in addition to co-staining steady state CLSM experiments, fluorescence lifetime imaging FLIM was used to follow the PS release from the HSA nanoparticles during their decomposition after endocytotic uptake (see results in Figs. 5 and 6).

The average of intracellular fluorescence lifetime of mTHPP applied without nanoparticles shortened from 9.0 ns observed for 5 h incubation to 8.1 ns for 24 h. This shift of the intracellular fluorescence lifetime is caused by a broadening of the spectrum of the detected lifetimes in the image of the cells (see Fig. 6).

This indicates an intracellular redistribution of mTHPP between 5 h and 24 h incubation. This effect is not fully understood yet and needs further investigations.

In contrast to the mTHPP incubated cells no change of fluorescence lifetime was detected in the cells treated with mTHPP-HSA nanoparticles over the whole incubation time.

The release of mTHPP from the HSA nanoparticles is not detectable via FLIM, even the CLSM measurement shows only a low PS amount applied with nanoparticles that is released from lysosomes after 24 h (see Fig. 4).

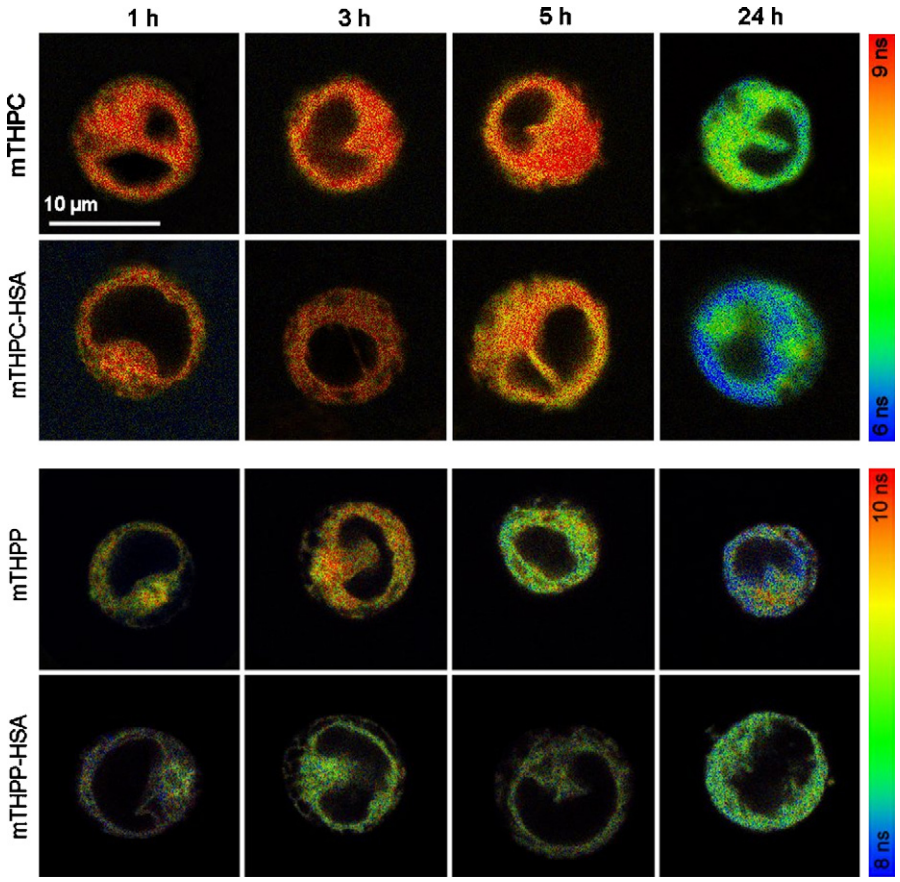

Fig. 5. FLIM pictures of PS distribution in Jurkat cells after 1 h, 3 h, 5 h, and 24 h incubation: mTHPC (first line), mTHPC-HSA nanoparticles (second line), mTHPP (third line) and mTHPP-HSA nanoparticles (fourth line). For all samples at least four cells were imaged, one representive image per sample is shown.

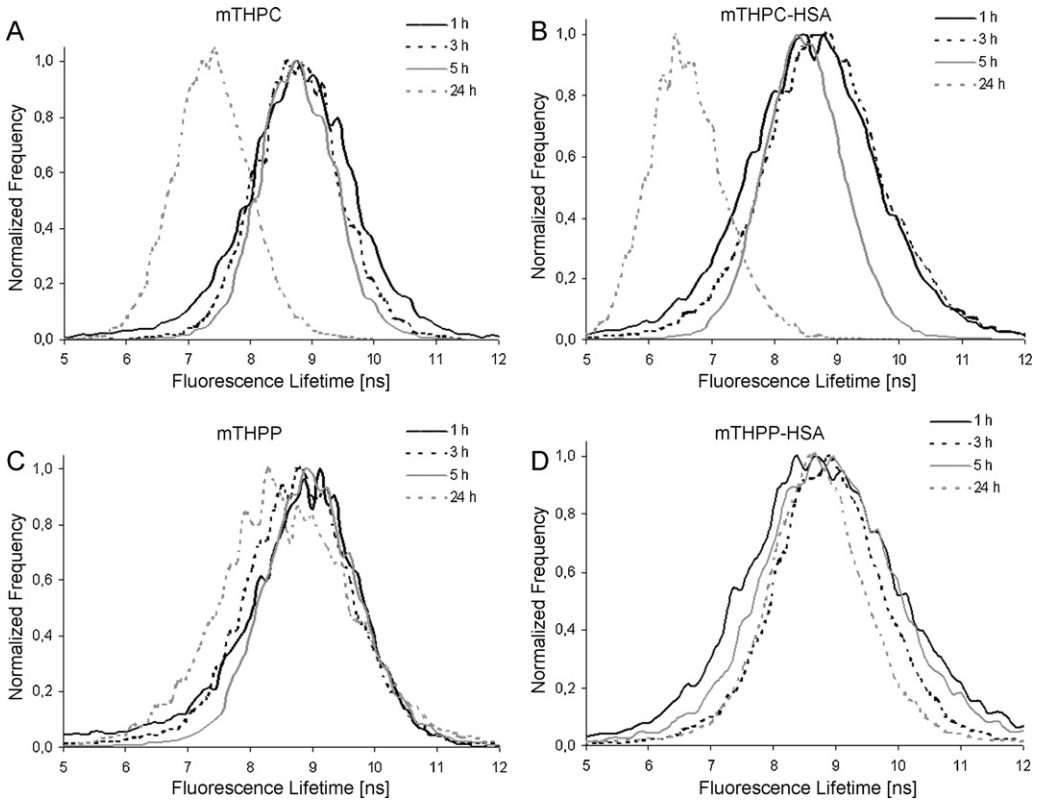

Fig. 6. Histograms of FLIM measurements of PSs inside Jurkat cells after 1 h, 3 h, 5 h, and 24 h incubation. The Jurkat cells are incubated with mTHPC (A), mTHPC-HSA nanoparticles (B), mTHPP (C) and mTHPP-HSA nanoparticles (D). For all samples at least four cells were imaged, the normalized sum of all measured histograms per cell is shown.

Table 2
$^1O_2$ generation and triplet parameters of mTHPP, mTHPC as well as mTHPP- and mTHPC-HSA nanoparticles in Jurkat cells. (a) Relative to the data of mTHPP; (b) relative to the data, of mTHPC. $^1O_2$ measurement in Jurkat cells: incubation time 5 h.

	τ_T [μs]	τ_Δ [μs]	Relative Φ_Δ
mTHPP	4.0 ± 1.0	0.80 ± 0.05	100%[a]
mTHPP-HSA	4.0 ± 1.0	0.70 ± 0.05	27.4%[a]
mTHPC	3.6 ± 1.0	0.65 ± 0.05	100%[b]
mTHPC-HSA	4.0 ± 1.0	0.60 ± 0.05	45.0%[b]

Coincident to the localization of mTHPC and mTHPC-HSA nanoparticles in lysosomes the fluorescence lifetime distribution also shows a similar behaviour (see Figs. 5 and 6). After 1 h, 3 h, and 5 h of incubation the average fluorescence lifetime of 9 ns does not change significantly. After 24 h it decreases to 6.2 ns for mTHPC-HSA nanoparticles and 7.2 ns for mTHPC, respectively.

The decrease of the mTHPC fluorescence lifetime in mTHPC-HSA nanoparticle treated cells is a consecution of the mTHPC release from the nanoparticles. In case of mTHPC applied without nanoparticles it should be related to the release from other proteins like serum albumin and the distribution of the PS in the cytoplasm. This observation is in agreement with the CLSM data showing the release of mTHPC from the lysosomes after 24 h (see Fig. 4).

3.4. Intracellular $^1O_2$ generation and triplet lifetime

To check the ability of the PS to generate $^1O_2$ in their intracellular microenvironment the $^1O_2$ generation after 5 h of incubation in Jurkat cells was measured. A detailed discussion of these data is given in Wacker et al. (2010). Here they are used for the comparative discussion with the results of the other *in vitro* experiments.

After 5 h of incubation, both mTHPP- and mTHPC-HSA nanoparticles generate $^1O_2$ inside Jurkat cells. The values of triplet lifetime of mTHPP and mTHPP-HSA in Jurkat cells are 4.0 μs (see Table 2). The values of $^1O_2$ lifetime are also similar: 0.8 μs for mTHPP and 0.7 μs for mTHPP-HSA nanoparticles, respectively. However, the intensity of intracellular $^1O_2$ luminescence of mTHPP-HSA nanoparticles is only one fourth compared to that of mTHPP (see Table 2). This result coincides with intracellular uptake (see Fig. 3).

The intracellular uptake data show that after 5 h of incubation, the amount of mTHPP-HSA nanoparticles taken up by Jurkat cells is less than that of mTHPP. The low intracellular uptake of mTHPP-HSA nanoparticles leads to less $^1O_2$ generation inside the Jurkat cells compared to mTHPC-HSA nanoparticles. The triplet lifetime of mTHPC in Jurkat cells (3.6 μs) is shorter than the intracellular triplet lifetime of mTHPP, mTHPP- and mTHPC-HSA nanoparticles (4.0 μs). However, the $^1O_2$ lifetime of mTHPC is nearly the same as for mTHPC-HSA nanoparticles (see Table 2).

In both cases the intracellular $^1O_2$ luminescence of the PS loaded nanoparticles is much lower than that of the PS applied without nanoparticles. That coincides with the observations of the drug release.

The intensity of intracellular $^1O_2$ luminescence of mTHPP-HSA nanoparticles is 27.4% compared to the value of the free mTHPP applied without nanoparticles. After 5 h of incubation no drug release of mTHPP-HSA was observed (see the FLIM images see Fig. 5 and the intracellular distribution see Fig. 4). The most mTHPP molecules are still attached to the HSA-nanoparticle surface, this causes a lower $^1O_2$ luminescence.

The intensity of intracellular $^1O_2$ luminescence generated by mTHPC-HSA nanoparticles is about 45% compared to the value of the mTHPC applied without nanoparticles. The CLSM images (see Fig. 4) show a faster drug release from the lysosomes for mTHPC applied without nanoparticles compared to mTHPC applied with HSA nanoparticles.

This effect is caused by the fact that in the first case the mTHPC is attached to single serum albumins whereas in the second case the PS is attached to large HSA nanoparticles. For this reason the time of the release of these different "carriers" is different. As a result the release from the lysosomes for mTHPC applied with HSA nanoparticles is delayed and causes a lower intracellular $^1O_2$ luminescence.

A high potential of mTHPC-HSA nanoparticles being an effective PS carrier system is allocated by the efficient drug release (see Figs. 5 and 6), the subsequent intracellular distribution (see Fig. 4) and the efficient $^1O_2$ generation (see Table 2) by the released PS.

3.5. Dark toxicity and phototoxicity

Beside the photophysical properties of the PS the photodynamic effect depends on the intracellular uptake, the drug release from the

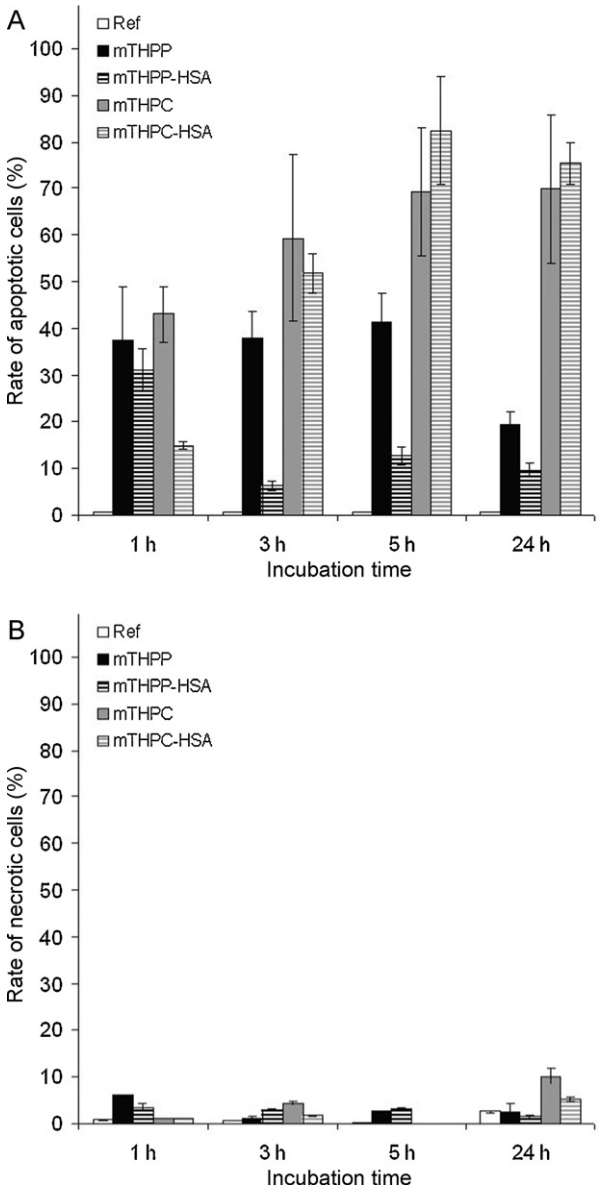

Fig. 7. Phototoxicity of 3 μM mTHPP, mTHPP-HSA nanoparticles, mTHPC, mTHPC-HSA nanoparticles in Jurkat cells after different incubation times. (A) Rate of apoptotic cells, (B) rate of necrotic cells. The experiments were repeated twice and for each measurement the cell number was counted three times to get an average. Error bars represent the standard deviation ($n = 6$). Jurkat cells cultured with medium were taken as reference (Ref.). The cells were irradiated with $\lambda_{ex} = 660$ nm for 120 s resulting 280 mJ/cm^2.

nanoparticles and the intracellular distribution of the PS. For this reason the dark and phototoxicity were investigated in dependence on incubation time. The different types of cell death, apoptosis and necrosis, were followed to characterize the phototoxic effects.

For all samples, independent of the application form and the uptake mechanism, apoptosis was found to be the main cell death pathway caused by both PS, mTHPP and mTHPC (see Fig. 7).

Proving the phototoxic effect the dark toxicity was measured, too. Without irradiation no significant rate of apoptosis was measured. For dark toxicity the rate of necrosis is less than 5% in the first 5 h and less than 8% after 24 h of incubation (data not shown). Thus, the rate of necrosis after irradiation is nearly the same as without irradiation.

The rate of apoptosis after irradiation in the samples treated with mTHPP without nanoparticles in the first 5 h is continual below 45% after 24 h incubation it decreases to 22%. The irradiated mTHPP-HSA nanoparticles treated cells show a rate of apoptosis of 32% after 1 h of incubation but only 8–12% after 3 h, 5 h, and 24 h of incubation.

The high phototoxicity of mTHPP and mTHPP-HSA nanoparticles after short incubation times is not clear yet. After incubation times longer than 1 h the phototoxicity of mTHPP-HSA is lowered compared to mTHPP and does not change with increasing time. This result is in good agreement with the observation of negligible mTHPP release from the nanoparticles over 24 h.

The maximum of phototoxicity of cells treated with mTHPC and mTHPC-HSA nanoparticles is reached after 5 h and keeps high after 24 h of incubation. The rate of apoptosis in these samples is between 70% and 85%.

After 5 h of incubation the most mTHPC molecules applied without nanoaprticles and a high amount of mTHPC molecules applied with HSA nanoparticles are released from the lysosomes. This drug release affects the efficiency of photosensitization much more than the increase of the intracellular PS concentration.

The much higher phototoxic efficiency of the mTHPC loaded nanoparticles in comparison to the mTHPP loaded nanoparticles coincides with their better uptake (see Fig. 3), as well as with their faster and complete drug release (see Figs. 4–6) and the resulting significant higher $^1O_2$ generation (see Table 2).

4. Conclusions

HSA nanoparticles are efficient drug carriers for porphyrin based PSs. HSA nanoparticles, loaded with mTHPP or mTHPC, are able to transport the PS into Jurkat cells.

The intracellular uptake of mTHPC-loaded nanoparticles is significantly more efficient than the intracellular uptake of mTHPP-loaded nanoparticles. The lysosomal decomposition of the HSA nanoparticles is faster for mTHPC-loaded than for mTHPP-loaded nanoparticles as well.

This result leads to the assumption that the PS and its interactions with the HSA nanoparticles and with the cellular structures can influence the velocity of the intracellular uptake and the drug release.

Due to its passive uptake free mTHPP unlike the mTHPP-loaded nanoparticles accumulates in Jurkat cells in the same amount like free mTHPC and mTHPC-loaded HSA nanoparticles. The detected endocytotic uptake confirms the stability of the PS loaded nanoparticles, as it was already shown in solution by Wacker et al. (2010).

In Jurkat cells the phototoxicity of mTHPC-loaded nanoparticles and of free mTHPC is much higher than that of the mTHPP-loaded nanoparticles and the free mTHPP.

The low phototoxicity of mTHPP-HSA nanoparticles is not exclusively caused by the lower uptake. Even the highly taken up free mTHPP shows a much lower phototoxicity than mTHPC. The low phototoxicity of mTHPP is probably caused by the much lower absorbance in the region of the excitation wavelength (660 nm) (Wacker et al., 2010) and the consequently much lower $^1O_2$ generation.

Additionally, the different amphiphilicity of the mTHPP and mTHPC molecules affects their ability of $^1O_2$ generation (Roeder et al., 2004; Rancan et al., 2005b).

HSA nanoparticles were found to be an acceptable carrier for mTHPP, too, but the behaviour of mTHPP is not satisfying. Due to its slow-down effect to the endocytotic uptake of the nanoparticles and to the nanoparticle decomposition the use of HSA nanoparticles seems not to be promising.

Because of strong interactions between PS molecules the $^1O_2$ generation of PS loaded on nanoparticles is much lower than for the PS without nanoparticles. Thus, the intracellular release of the PS from the nanoparticles causing their monomerisation is a precondition for its photoactivity. As a result of the release process after light absorption $^1O_2$ can be generated.

For this reason the HSA nanoparticles are potential very powerful carriers for PS since they are “inactive” until the release from the nanoparticles inside of the target cells.

Acknowledgements

The authors want to acknowledge BMBF (Bundesministerium für Bildung und Forschung; Project 0312026A) for financial support and Biolitec AG Jena for reagent supply. The authors also thank Lutz Jäger of the Department of Physics, Humboldt-Universität zu Berlin, for technical assistance and Dr. Korte of the Department of Biology, Humboldt-Universität zu Berlin, for technical support on CLSM and FLIM.

References

Amato, I., 1993. Cancer therapy. Hope for a magic bullet that moves at the speed of light. Science 262, 32–33.

Bento-Abreu, A., Velasco, A., Polo-Hernández, E., Lillo, C., Kozyraki, R., Tabernero, A., Medina, J.M., 2009. Albumin endocytosis via megalin in astrocytes is caveola- and Dab-1 dependent and is required for the synthesis of the neurotrophic factor oleic acid. J. Neurochem. 111, 49–60.

Bonnett, R., White, R., Winfield, U., Berenbaum, M., 1989. Hydroporphyrins of the meso-tetra(hydroxyphenyl)porphyrin series as tumour photosensitizers. Biochem. J. 261, 277–280.

Chen, K., Preuß, A., Hackbarth, S., Wacker, M., Langer, K., Röder, B., 2009. Novel photosensitizer-protein nanoparticles for photodynamic therapy: photophysical characterization and in vitro investigations. J. Photochem. Photobiol. B: Biol. 96, 66–74.

Chen, K., Wacker, M., Hackbarth, S., Langer, K., Roeder, B., 2010. Photophysical evaluation of mTHPC-loaded HSA nanoparticles as novel PDT delivery systems. J. Photochem. Photobiol. Biol.: B.

Copper, M., Tan, I., Oppelaar, H., Ruevekamp, M., Stewart, F., 2003. Metatetra(hydroxyphenyl)chlorin photodynamic therapy in earlystage squamous cell carcinoma of the head and neck. Arch. Otolaryngol. Head Neck Surg. 129, 709–711.

Dougherty, T., Gomer, C., Henderson, B., Jori, G., Kessel, D., Korbelik, M., Moan, J., Peng, Q., 1998. Photodynamic Therapy. J. Natl. Cancer Inst. 90, 889–905.

Dreis, S., Rothweiler, F., Michaelis, M., Cinatl, J., Kreuter, J., Langer, K., 2007. Preparation, characterisation and maintenance of drug efficacy of doxorubicin-loaded human serum albumin (HSA) nanoparticles. Int. J. Pharm. 341, 207–214.

Duncan, R., Sat, Y.N., 1998. Tumor targeting by enhanced permeability and retention (EPR) effect. Ann. Oncol. 9, 39–52.

Foote, C.S., 1968. Mechanisms of photosensitized oxidation. there are several different types of photosensitized oxidation which may be important in biological systems. Science 162, 963–970.

Gelperina, S., Kisich, K., Iseman, M.D., Heifets, L., 2005. The potential advantages of nanoparticle drug delivery systems in chemotherapy of tuberculosis. Am. J. Respir. Crit. Care Med. 172, 1487–1490.

Henderson, B., Dougherty, T., 1992. How does photodynamic therapy work? Photochem. Photobiol. 55, 145–157.

Hopper, C., Kubler, A., Lewis, H., Tan, I., Putnam, G., 2004. mthpc mediated photodynamic therapy for early oral squamous cell carcinoma. Int. J. Cancer 111, 138–146.

Jux, N., Röder, B., 2010. Handbook of porphyrin science. Vol. 4, Phototherapy, Radioimmunotherpay and Imaging. In: Targeting Strategies for tetrapyrrole-based Photodynamic Therapy. World Scientific Publishing Co. Pte. Ltd, Singapore.

Kessel, D., Luo, Y., 1998. Mitochondrial photodamage and PDT-induced apoptosis. J. Photochem. Photobiol. B 42, 89–95.
Langer, K., Anhorn, M., Steinhauser, I., Dreis, S., Celebi, D., Schrickel, N., Faust, S., Vogel, V., 2008. Human serum albumin (HSA) nanoparticles: reproducibility of preparation process and kinetics of enzymatic degradation. Int. J. Pharm. 347, 109–117.
Langer, K., Coester, C., von Briesen, H., Kreuter, J., 2000. Preparation of avidin-labeled protein nanoparticles as carriers for biotinylated peptide nucleic acid (PNA). Eur. J. Pharm. Biopharm. 49, 303–307.
Leung, W.N., Sun, X., Mak, N.K., Yow, C.M., 2002. Photodynamic effects of mTHPC on human colon adenocarcinoma cells: photocytotoxicity, subcellular localization and apoptosis. Photochem. Photobiol. 75, 406–411.
Ma, L., Moan, J., Berg, K., 1994. Evaluation of a new photosensitizer, meso-tetrahydroxyphenyl-chlorin, for use in photodynamic therapy: a comparison of its photobiological properties with those of two other photosensitizers. Int. J. Cancer 57, 883–888.
Maeda, H., 1994. Polymer conjugated macromolecular drugs for tumor-specific targeting. In: Polymeric Site-specific Pharmacotherapy. John Wiley & Sons, Inc., New York, pp. 96–116.
Maeda, H., Sawaa, T., Konno, T., 2001. Mechanism of tumor-targeted delivery of macromolecular drugs, including the EPR effect in solid tumor and clinical overview of the prototype polymeric drug SMANCS. J. Control. Release 74, 47–61.
Marchal, S., Bezdetnaya, L., Guillemin, F., 2004. Modality of cell death induced by foscan-based photodynamic treatment in human colon adenocarcinoma cell line HT29. Biochemistry (Mosc) 69, 45–49.
Matsamura, Y., Maeda, H., 1986. A new concept for macromolecular therapeutics in cancer chemotherapy: mechanisms of tumoritropic accumulation of protein and the antitumor agent SMANCS. Cancer Res. 46, 6387–6392.
Oelckers, S., Ziegler, T., Michler, I., Röder, B., 1999. Time-resolved detection of singlet oxygen luminescence in red-cell ghost suspensions: concerning a signal component that can be attributed to singlet oxygen luminescence from the inside of a native membrane. J. Photochem. Photobiol. B: Biol. 53, 121–127.
Oleinick, N.L., Morris, R.L., Belichenko, I., 2002. The role of apoptosis in response to photodynamic therapy: what, where, why, and how. Photochem. Photobiol. Sci. 1, 1–21.
Paul, A., Hackbarth, S., Mölich, A., Luban, C., Oelckers, S.F., Böhm a, d.B.R., 2003. Comparative study of the photosensitization of Jurkat cells in vitro by pheophorbide-a and a pheophorbide-a diaminobutane poly-propylene-imine dendrimer complex. Laser Phys. Vol.13, 22–29.
Paul, A., Mölich, A., Oelckers, S.M., Seifert, B.R., 2002. Alkyl-substituted magnesium phthalocyanine: phototoxicity after excitation of higher electronic states in cells in vitro. J. Porphyrins Phthalocyanines 6, 340–346.
Perrault, S.D., Walkey, C., Jennings, T., Fischer, H.C., Chan, W.C.W., 2009. Mediating tumor targeting efficiency of nanoparticles through design. Nano Lett. 9, 1909–1915.
Rancan, F., Helmreich, M., Moelich, A., Jux, N., Hirsch, A., Roeder, B., Witte, C., Boehm, F., 2005a. Fullerene-pyropheophorbide a complexes as sensitizer for photodynamic therapy: uptake and photo-induced cytotoxicity on Jurkat cells. J. Photochem. Photobiol. B: Biol. 80, 1–7.
Rancan, F., Wiehe, A., Noebel, M., Senge, M.O., Omari, S.A., Boehm, F., John, M., Roeder, B., 2005b. Influence of substitutions on asymmetric dihydroxychlorins with regard to intracellular uptake, subcellular localization and photosensitization of Jurkat cells. J. Photochem. Photobiol. B: Biol. 78, 17–28.
Röder, B., 2000. Photodynamic therapy. In: Encyclopedia Analytical Chemistry. John Wiley & Sons Ltd., Chichester, pp. 302–320.
Roeder, B., Ermilov, E.A., Hackbarth, S., Helmreich, M., Jux, N., 2006. Trap formation and energy transfer in pheophorbide a -DAB-dendrimers and pyropheophorbide a – fullerene C60 hexaadduct molecular systems. SPIE 6192, 495–507.
Roeder, B., Hackbarth, S., Wiehe, A., Rancan, F., Jux, N., und Andreas Hirsch, M.H., Ermilov, E., Senge, M.O., Noebel, M., Omari, S.A., Simonenko, K., 2004. Influence of tetra pyrrole amphiphicility on membrane localization and the mechanism of photosensitized cell death. J. Porphyrins Phthalocyanines 8, 472.
Sasnouski, S., Zorin, V., Khludeyev, I., D'Hallewin, M.-A., Guillemin, F., Bezdetnaya, L., 2005. Investigation of foscan interactions with plasma proteins. Biochim. Biophys. Acta 1725, 394–402.
Schlothauer, J., Hackbarth, S., Röder, B., 2008. A new benchmark for time-resolved detection of singlet oxygen luminescence – revealing the evolution of lifetime in living cells with low dose illumination. Laser Phys. Lett. 6, 216–221.
Tabernero, A., Velasco, A., Granda, B., Lavado, E.M., Medina, J.M., 2002. Transcytosis of albumin in astrocytes activates the sterol regulatory element-binding protein-1, which promotes the synthesis of the neurotrophic factor oleic acid. J. Biol. Chem. 277, 4240–4246.
Wacker, M., Chen, K., Preuss, A., Possemeyer, K., Röder, B., Langer, K., 2010. Photosensitizer loaded HSA nanoparticles (part I): preparation and photophysical properties. Int. J. Pharm..
Willingham, M.C., Pastan, I., 1984. Endocytosis and exocytosis: current concepts of vesicle traffic in animal cells. Int. Rev. Cytol. 92, 51–92.